hydrogen

MDPI

Article

Role of Ultrasonic Shot Peening in Environmental Hydrogen Embrittlement Behavior of 7075-T6 Alloy

Mahdieh Safyari [1,2,*] and Masoud Moshtaghi [3,*]

[1] Institute for Materials Research, Tohoku University, 2-1-1 Katahira, Aoba-Ku, Sendai 980-8577, Japan
[2] Graduate School of Engineering, Tohoku University, Aramaki Aza Aoba 6-6, Aoba-Ku, Sendai 980-8579, Japan
[3] Department of General and Analytical Chemistry, University of Leoben, Franz Josef-Straße 18, 8700 Leoben, Austria
* Correspondence: safyari@imr.tohoku.ac.jp (M.S.); masoud.moshtaghi@unileoben.ac.at (M.M.)

Abstract: The effect of ultrasonic shot peening on the environmental hydrogen embrittlement behavior of the 7075-T6 aluminum alloy is investigated. The 7075-T6 tensile specimens were treated by ultrasonic shot peening for 50 s. Surface residual stress and the depth of residual stress under the surface were evaluated using an X-ray diffractometer. Then, the specimens were tensile tested in humid air and dry nitrogen gas by the slow strain rate technique. The results showed that the ultrasonic shot-peened specimen has a superior hydrogen embrittlement resistance. Further, the ultrasonic shot peening changes the fracture mode from an intergranular fracture mode to the transgranular one. It was suggested that ultrasonic shot-peening has two effects on hydrogen embrittlement behavior; the distribution of hydrogen inside the surface layer by introducing dislocations/vacancies as hydrogen traps and reducing the normalized amount of hydrogen trapped per unit length of the grain boundary.

Keywords: aluminum alloy; hydrogen embrittlement; ultrasonic shot peening; transgranular fracture; intergranular fracture

Citation: Safyari, M.; Moshtaghi, M. Role of Ultrasonic Shot Peening in Environmental Hydrogen Embrittlement Behavior of 7075-T6 Alloy. *Hydrogen* **2021**, *2*, 377–385. https://doi.org/10.3390/hydrogen2030020

Academic Editor: George E. Marnellos

Received: 15 August 2021
Accepted: 10 September 2021
Published: 11 September 2021

1. Introduction

Advanced materials are essential for boosting the fuel economy of modern automobiles while maintaining safety and performance. Because it takes less energy to accelerate a lighter object than a heavier one, lightweight materials offer a great potential for increasing vehicle efficiency. Replacing cast iron and traditional steel components with lightweight materials such as high-strength 7xxx series aluminum (Al) alloys can directly reduce the weight of a vehicle's body and chassis by up to 50 percent and, therefore, reduce the fuel consumption of a vehicle [1–4]. Materials used in automobile components may encounter challenges from high stress in environments with a humidity of more than 40% [5]. Such service conditions require structural materials to possess both high strength and good hydrogen embrittlement (HE) resistance. The problems of environmentally assisted cracking in humid environments were reported for the aluminum alloys [5–10]. Thus, considerable studies have been conducted to develop a high-strength HE-resistant aluminum alloy through the optimization of alloy composition and heat treatment.

Various mechanical surface treatments have been developed to produce a nanostructured layer on the top surface of metal materials such as high-pressure torsion [11,12], roller burnishing [13], surface mechanical attrition treatment [14,15], shot peening [16,17] and ultrasonic shot peening [18]. Among these techniques, shot peening is one of the most usual processes for a high productivity, low cost, and flexibility in the sample shape [19]. Shot peening and, also, ultrasonic shot peening involve the repeated impact of hard balls on the surface of the specimen. In comparison with the conventional shot peening method, ultrasonic shot peening produces a compressive residual stress layer and work hardening in a larger depth along with the formation of nanostructure in the surface region because

of the high kinetic energy associated with the hard balls in this process [20]. These results in a further modification in the mechanical properties of aluminum alloys by the ultrasonic shot peening process compared with the conventional shot peening.

Recently, many works have been conducted to investigate the properties of the surface layers produced by shot peening on Al alloys [21–25]. Researchers reported the positive effect of compressive residual stress and nanocrystallization on the hardness, fatigue properties, and anodic corrosion behavior. For instance, Benedetti et al. [21] investigated the effect of the shot peening on the high and very-high cycle plain fatigue resistance of the Al-7075-T651 alloy. They showed that shot peening conducted at low intensities with small beads is more effective in incrementing the fatigue resistance as compared to more intense treatments with larger shots since it causes a lower surface roughening and induces the maximum compressive residual stress as close as possible to the surface. Further, Cho et al. [25] demonstrated that after shot peening, the surface hardness increases more than twice that of the base material. However, studies on the hydrogen embrittlement behavior of materials with shot-peened surface layers are quite limited in aluminum alloys. To better understand the effect of a shot-peen-treated surface on the hydrogen embrittlement resistance of Al alloys, the ultrasonic shot peening process was chosen to produce a nanostructured surface layer on a commercial aluminum alloy, 7075-T6 in this investigation, and the hydrogen-induced mechanical degradation was evaluated by a tensile test at a low strain rate in humid air.

2. Materials and Methods

In this experiment, commercially available 7075-T6 aluminum alloy was used for preparing tensile test specimens with the gauge dimension of 1 mm × 5 mm × 12 mm. The chemical composition of the materials is presented in Table 1.

Table 1. Chemical composition of the 7075 Al alloy (wt%).

Zn	Mg	Cu	Si	Fe	Cr	Al
4.76	2.05	1.61	0.31	0.006	0.12	Bal

The ultrasonic shot peening (Stressonic®, SONATS, Carquefou, France) was carried out on each surface of the tensile specimen using hard steel balls of 160 µm diameter with a hardness of 60 HRC at a constant amplitude of 80 µm for 50 s. The residual stress distribution introduced by ultrasonic shot peening was assessed using Rigaku X-ray diffractometer (XRD) operating with Cu Kα radiation at 40 kV and 30 mA and using the $\mathrm{Sin}^2\omega$ method (the method has been previously described elsewhere [26–30]). The measurement direction was the longitudinal direction of the specimen. The depth distribution of the residual stress was obtained after electrolytic polishing of the specimens with the dimension of 1 mm × 5 mm × 5 mm.

The effect of hydrogen on the mechanical properties was evaluated by slow strain-rate tensile tests (SSRTs, SINGO) [31] at a rate of 10^{-5} min^{-1}. The ultrasonic shot-peened and unshot-peened specimens were tested under two conditions, i.e., humid air with 90% humidity (HA) and dry nitrogen gas (DNG) as a reference environment. To quantify HE resistivity, the total elongation loss (δ_{loss}) was defined as follows [5,6]:

$$\delta_{loss} = \frac{\delta_{DNG} - \delta_{HA}}{\delta_{DNG}} \times 100 \quad (1)$$

where δ_{DNG} and δ_{HA} are the elongation of the specimens which were tested in DNG and HA, respectively. Hydrogen embrittlement sensitivity increased with increasing δ_{loss}. Several factors such as temperature, rate of loading, stress concentrations, microstructural characteristics, heat treatment and size of the specimen can alter the fracture behaviors of the metallic materials [32–35]. For investigation of the effect of ultrasonic shot peening on

the fracture behavior of the alloy in different environments, the fractured specimens were characterized using a scanning electron microscope (SEM).

3. Results and Discussion

The residual stresses induced in the ultrasonic shot-peened specimen as a function of the distance from the surface are shown in Figure 1. Residual stresses formed during the ultrasonic shot peening were found to be compressive and the magnitude of stress in 7075-T6 alloy ranged from 0 to −160 MPa. The magnitude of compressive stress decreased with increasing the distance from the surface. The results also indicated that the compressive residual stress was observed in the depth of about 100 μm from the surface.

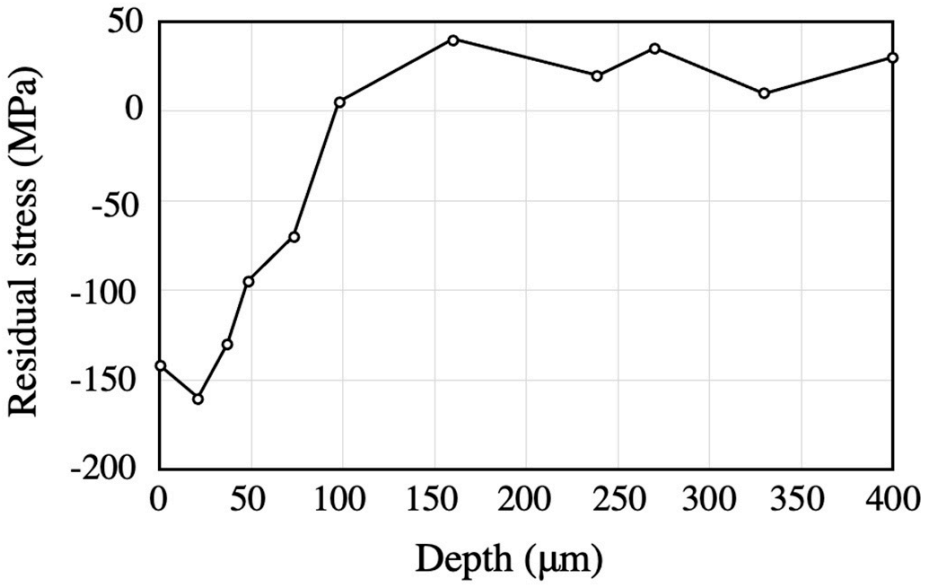

Figure 1. Depth profile of residual stress of shot-peened specimen.

Figure 2 shows the tensile test specimen and the nominal stress–nominal strain curves of the ultrasonic shot-peened and the unshot-peened specimens which were deformed in DNG. Both specimens showed high total elongation values (close to 10%). These values are considered to be representative of the intrinsic tensile elongation value which was not affected by the environment. Further, Figure 2b showed that the yield and flow stresses of the ultrasonic shot-peened specimen were higher than those of the unshot-peened specimen, while the total elongation value of the ultrasonic shot-peen treated specimen was lower than that of the unshot-peened specimen. These features can be ascribed to the shot-peened surface layer in which high work hardening contributes to the behavior of flow stress, elongation, and fracture. Particularly, the micro-cracks at the specimen surface may lead to a premature failure in the ultrasonic shot-peened specimen.

Figure 3 shows nominal stress–nominal strain curves of both specimens which were tested in HA. It was clear that the total elongation of both specimens was low in comparison with those of the specimens which were tested in DNG. This result appeared to be consistent with the results reported in previous studies [5,6,8,36–39]; the 7075-T6 alloy is very susceptible to environmental hydrogen embrittlement at room temperature. The results of SSRTs are summarized in Table 2. As can be seen in Table 2, compared to the unpeened specimen, the total elongation of the shot-peened specimen tested in HA was not significantly reduced from that of the specimen deformed in the DNG. Figure 4 shows the obtained δ_{loss} for the specimens. These results indicate that the environmental hydrogen embrittlement of 7075-T6 alloy was mitigated by ultrasonic shot peening.

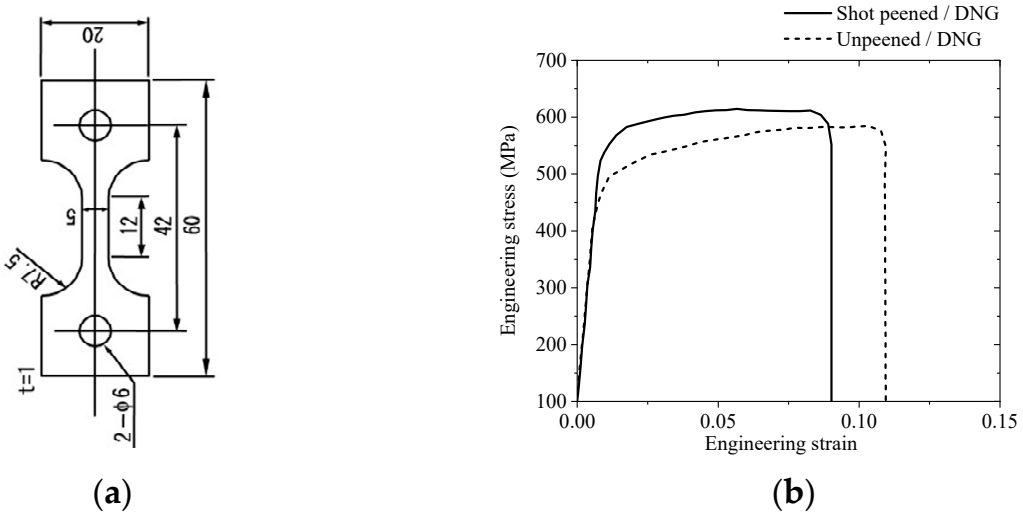

Figure 2. (**a**) Tensile test specimen cut from the 7075 aluminum alloy, (**b**) representative tensile stress–strain curves of the specimens which were tested in dry nitrogen gas (DNG) at strain rate of 10^{-5} min^{-1}.

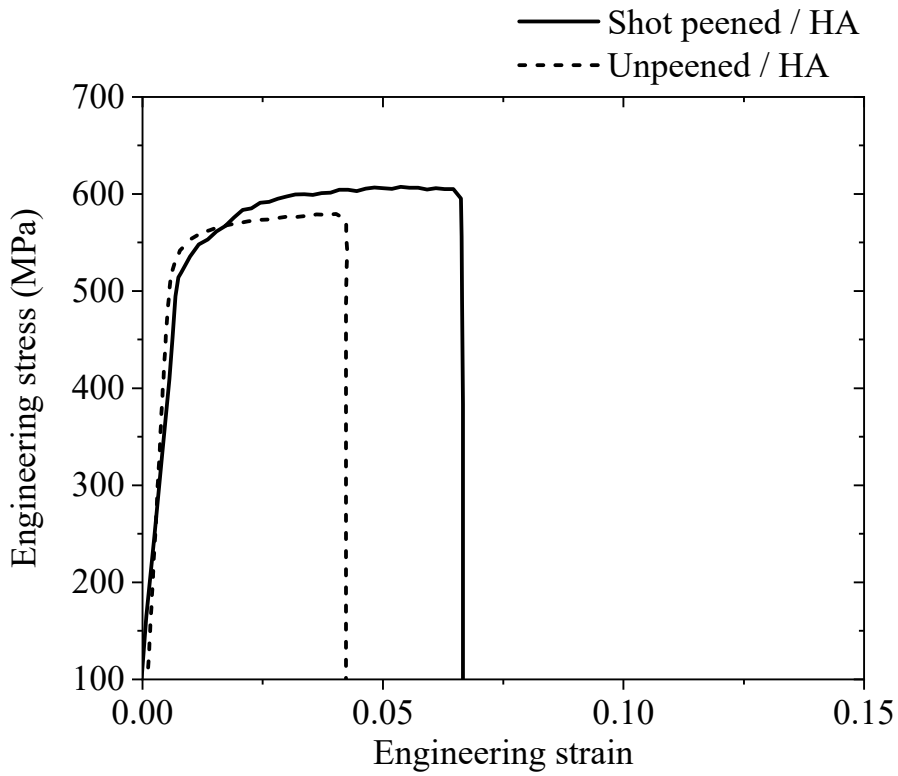

Figure 3. Representative tensile stress–strain curves of the specimens which were tested in humid air (HA) at strain rate of 10^{-5} min^{-1}.

Table 2. The results of SSRTs were conducted under various environments.

Specimen	Environment	Ultimate Tensile Strength (MPa)	Elongation (%)
Shot-peened	DNG	611.6	8.9
	HA	607.25	6.6
Unpeened	DNG	584.7	11.0
	HA	578.4	4.2

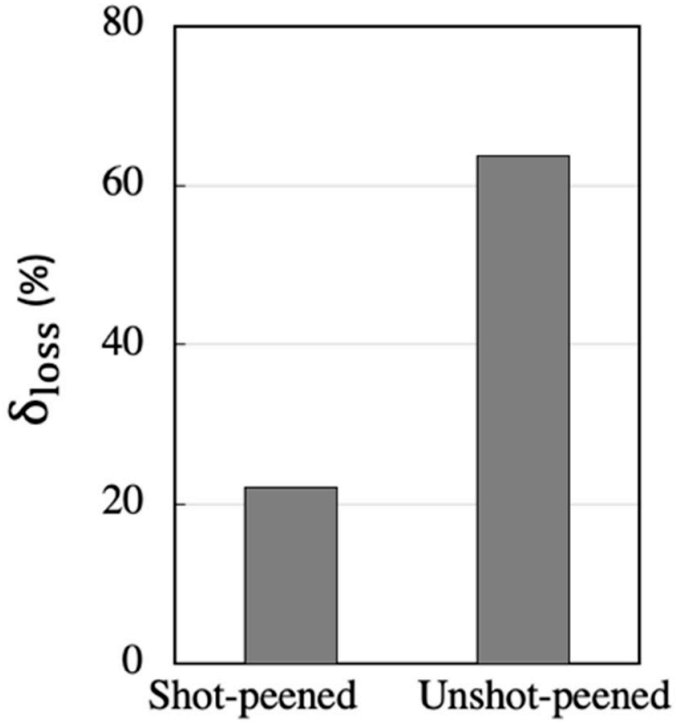

Figure 4. Calculated hydrogen embrittlement sensitivity index (δ_{loss}) of the specimens.

Figure 5 shows SEM fractography of the specimens which were tensile tested in HA. The fracture surface of the unshot-peened specimen was entirely covered by brittle fracture features, including grain boundary facets. The fracture surface of the ultrasonic shot-peened specimen, consisted of the transgranular fracture mode in the region near the surfaces; however, the fracture mode changed to the brittle intergranular fracture when approaching the center of the fracture surface. The width of the transgranular fracture region was measured to be about 95 μm from Figure 5b. This value was similar to the value which corresponded to the depth of residual stress of the specimen evaluated by the XRD measurement (see Figure 1). Thus, it is suggested that the ultrasonic shot peen treatment can mitigate the environmental hydrogen embrittlement, via changing the fracture mode from the intergranular to the transgranular fracture.

There were some possibilities that the hydrogen embrittlement behavior of the alloy 7075-T6 was affected by ultrasonic shot peening: (i) After ultrasonic shot peening, due to the severe deformation, the surface layer contained a high density of the dislocations and vacancies. Further, the complex deformation driven by the ultrasonic shot peening most likely introduced tangled cells or intersected dislocations rather than the dislocation pile ups [39,40]. The dislocations and vacancies are known as hydrogen trap sites in aluminum alloys [41]. Thus, the absorbed hydrogen could be trapped in the dislocations or the vacancies immediately after absorbing into the specimen from the surface during testing in HA. Therefore, the content of the trapped hydrogen at grain boundaries became low below the critical hydrogen content [42], causing the intergranular fracture. Moreover, it is understood that a transgranular fracture is induced by the presence of hydrogen in dislocations/vacancies [43]. Therefore, the observation of the transgranular fracture mode in the shot-peened region strengthened this hypothesis that hydrogen was mainly trapped at dislocation/vacancies in the shot-peen-treated region, meaning that ultrasonic shot peening can suppress hydrogen embrittlement by controlling trap site densities and hydrogen distribution.

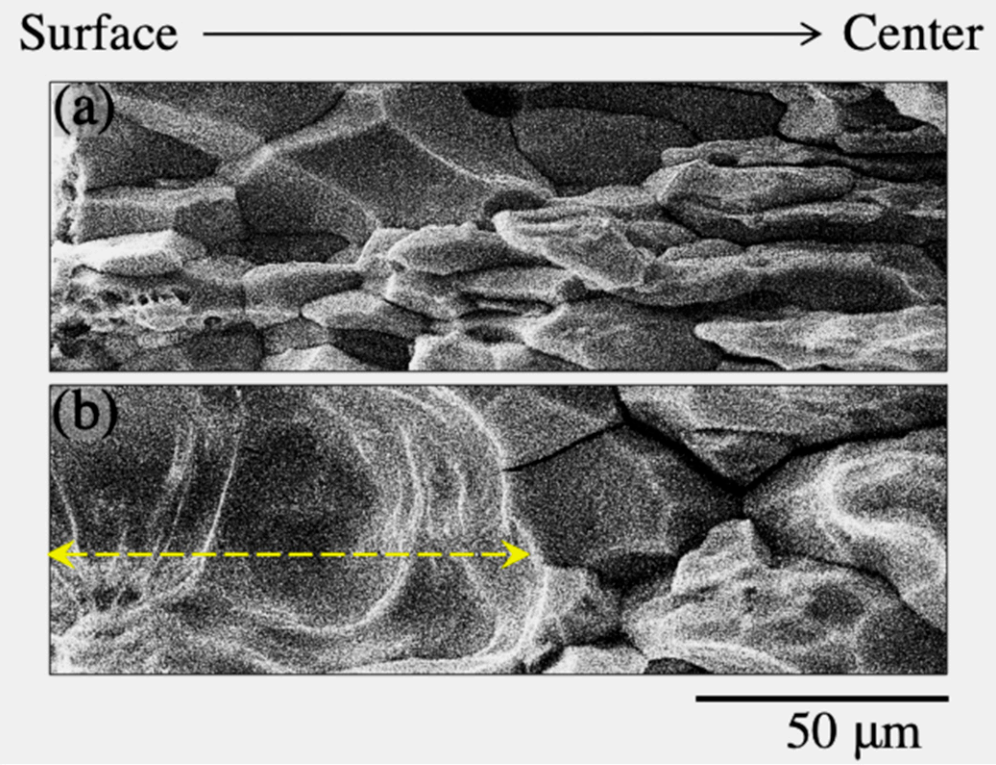

Figure 5. SEM fractography of the specimens which were deformed in humid air; (**a**) unshot-peened, and (**b**) the ultrasonic shot-peened specimens. The yellow arrow indicates the width of the transgranular fracture.

(ii) Ultrasonic shot peening introduced compressive residual stress into the region near the surface (Figure 1). It was reported that the residual stress in 7xxx or 2xxx series aluminum alloys is effective in enhancing the mechanical properties of the alloys, especially fatigue properties, as it increases the cyclic lifetime [21–25]. This improvement in mechanical properties has been attributed to the inhabitation of crack initiation or early crack propagation by compressive stress field induced by ultrasonic shot peening. However, the obtained results in the present study showed that the total elongation was reduced by ultrasonic shot peening, indicating the lower ductility of the shot-peened specimen. Furthermore, it was suggested [44] that introducing compressive residual stress by shot peening reduces the lattice spacing that leads to reduce the diffusion of hydrogen from the environment into the alloy; thus, hydrogen embrittlement can be suppressed by reducing the hydrogen content and inhibiting the local hydrogen concentration at potential flaws, including the grain boundaries. However, it is well-known that the hydrogen cannot diffuse into aluminum alloys at room temperatures [45], indicating that the beneficial effect of compressive residual stress on hindering the diffusion was not applicable to the present study.

(iii) Tao et al. [46] showed that after ultrasonic shot peening treatments, the initial coarse-grained structure in the surface layer was refined into equiaxed ultrafine grains with random crystallographic orientations and the grain size increased with an increment of the distance from the peened surface. The grain size refinement by severe deformation results in an increase in the high angle grain boundaries area [41]. The grain boundaries blocked the dislocation movement during SSRT and, therefore, the grain size refinement played an important role in preventing dislocation-induced hydrogen transport. Further, the increase in grain boundary area led to distributing more of the hydrogen trapped in the grain boundary and reducing the normalized amount of hydrogen trapped in the unit length of the grain boundary, decreasing the possibility of building up a critical

hydrogen concentration required for intergranular crack initiation in a typical high-angle grain boundary.

Based on the above discussion, it is inferred that the ultrasonic shot-peening had two effects on hydrogen embrittlement behavior of the 7075-T6 alloy; the distribution of hydrogen inside the surface layer by introducing a high dislocation/vacancy density as hydrogen traps and increasing the grain boundary area. Hydrogen was distributed among trap sites in accordance with the trap site density and the occupancy derived by the binding energy at each trap site. Traps are characterized due to their interaction with hydrogen atoms and binding energy, i.e., reversible or irreversible. Dislocations are reversible traps, while vacancies and grain boundaries are irreversible trap sites. Due to the low binding energy, dislocations can act as hydrogen sources and a part of their hydrogen content can easily escape to other trap sites or flaws such as the grain boundary. In the present ultrasonic shot-peened specimen, the higher grain boundary area in the surface layer resulted in reducing the number of hydrogen atoms per unit length of high angle grain boundaries. As mentioned above, this prevented the grain boundaries from reaching a critical hydrogen concentration value required for intergranular crack nucleation. Therefore, the grain refinement in the surface layer by ultrasonic shot peening and increasing the total length of grain boundaries played a more critical role in the suppression of hydrogen embrittlement in the 7075-T6 alloy.

4. Conclusions

The nanostructured surface layer was prepared on the top surface of the 7075-T6 alloy by ultrasonic shot peening. The effect of this layer was investigated using SSRT in HA and DNG.

The major conclusions of the study are as follows:

1. The total elongation of the 7075-T6 alloy was drastically reduced in HA. However, when the specimen was shot-peen-treated, the total elongation was slightly reduced.
2. The shot-peened surface layer changed the fracture mode from intergranular to transgranular, leading to the mitigation of hydrogen embrittlement by ultrasonic shot peening.
3. The ultrasonic shot peening treatment decreased the grain size in the surface layer resulting in an increase in the grain boundary area and a decrease in the number of atomic hydrogen trapped per unit length of the grain boundary. Therefore, the fine-grained layer increased the hydrogen embrittlement resistance of the alloy.

Author Contributions: Conceptualization, M.S. and M.M.; methodology, M.S. and M.M.; software, M.S. and M.M.; validation, M.S. and M.M.; formal analysis, M.S. and M.M.; investigation, M.S. and M.M.; resources, M.S. and M.M.; data curation, M.S. and M.M.; writing—original draft preparation, M.S.; writing—review and editing, M.M.; visualization, M.S. and M.M.; supervision, M.M.; project administration, M.S. and M.M.; funding acquisition, M.S. and M.M. Both authors have read and agreed to the published version of the manuscript.

Funding: M. Safyari gratefully acknowledges the financial support of the Kamei Corporation, Japan.

Acknowledgments: The authors appreciate the helpful discussion and resources provided by S. Kuramoto and F. Abbasi.

Conflicts of Interest: The authors declare no conflict of interest.

References

1. Carle, D.; Blount, G. The suitability of aluminum as an alternative material for car bodies. *Mater. Des.* **1999**, *20*, 267–272. [CrossRef]
2. Hirsch, J. Recent development in aluminum for automotive applications. *Trans. Nonfer. Met. Soc. China* **2014**, *24*, 1995–2002. [CrossRef]
3. Ghassemi, M.H.; Abouei, V.; Moshtaghi, M.; Noghani, M.T. The effect of removing worn particles by ultrasonic cleaning on the wear characterization of LM13 alloy. *Surf. Eng. Appl. Electrochem.* **2015**, *51*, 382–388. [CrossRef]
4. Miller, M.S.; Zhuang, L.; Bottema, J.; Wittebrood, A.J.; de Smet, P.; Haszler, A.; Vieregge, A. Recent development in aluminum alloys for the automotive industry. *Mater. Sci. Eng. A* **2000**, *280*, 37–49. [CrossRef]

5. Kuramoto, S.; Okahana, J.; Kanno, M. Hydrogen assisted intergranular crack propagation during environmental embrittlement in an Al-Zn-Mg-Cu Alloy. *Mater. Trans.* **2001**, *42*, 2140–2143. [CrossRef]
6. Safyari, M.; Moshtaghi, M.; Kuramoto, M. Environmental hydrogen embrittlement associated with decohesion and void formation at soluble coarse particles in a cold-rolled Al–Cu based alloy. *Mater. Sci. Eng.* **2021**, *799*, 139850. [CrossRef]
7. Holroyd, N.J.H.; Hardie, D. Strain-rate effects in the environmentally assisted fracture of a commercial high-strength aluminum alloy (7049). *Corros. Sci.* **1981**, *21*, 129–144. [CrossRef]
8. Moshtaghi, M.; Safyari, M.; Hojo, T. Effect of solution treatment temperature on grain boundary composition and environmental hydrogen embrittlement of an Al-Zn-Mg-Cu alloy. *Vacuum* **2021**, *184*, 109937. [CrossRef]
9. Qiu, Y.; Yang, H.; Tong, L.; Wang, L. Research Progress of Cryogenic Materials for Storage and Transportation of Liquid Hydrogen. *Metals* **2021**, *11*, 1101. [CrossRef]
10. Safyari, M.; Moshtaghi, M.; Kuramoto, S. On the role of traps in the microstructural control of environmental hydrogen embrittlement of a 7xxx series aluminum alloy. *J. Alloy. Compd.* **2020**, *855*, 157300. [CrossRef]
11. Xu, C.; Horita, Z.; Langdon, T.G. The evolution of homogeneity in processing by high-pressure torsion. *Acta Mater.* **2007**, *55*, 203–212. [CrossRef]
12. Xu, C.; Horita, Z.; Langdon, T.G. The evolution of homogeneity in an aluminum alloy processed using high-pressure torsion. *Acta Mater.* **2008**, *56*, 5168–5176. [CrossRef]
13. Al-Qawabeha, U.F.; Al-Qawabah, S.M. Effect of roller burnishing on pure aluminum alloyed by copper. *Ind. Lubr. Tribol.* **2013**, *65*, 71–77. [CrossRef]
14. Chang, H.W.; Kelly, P.M.; Shi, Y.N.; Zhang, M.X. Thermal stability of nanocrystallized surface produced by surface mechanical attrition treatment in aluminum alloys. *Surf. Coat. Technol.* **2012**, *206*, 3970–3980. [CrossRef]
15. Sharp, P.K.; Clark, G. *The Effect of Peening on the Fatigue Life of 7050 Aluminium Alloy*; DSTO-RR-0208; Defense Science and Technology Organisation: Canberra, Australia, 2001.
16. Ye, Z.; Liu, D.; Zhang, X.; Wu, Z.; Long, F. Influence of combined shot peening and PEO treatment on corrosion fatigue behavior of 7A85 aluminum alloy. *App. Surf. Sci.* **2019**, *486*, 72–79. [CrossRef]
17. Chung, Y.-H.; Chen, T.-C.; Lee, H.-B.; Tsay, L.-W. Effect of Micro-Shot Peening on the Fatigue Performance of AISI 304 Stainless Steel. *Metals* **2021**, *11*, 1408. [CrossRef]
18. Pandey, V.; Rao, G.S.; Chattopadhyay, K.; Santhi Srinivas, N.C.; Singh, V. Effect of surface nanostructuring on LCF behavior of aluminum alloy 2014. *Mater. Sci. Eng. A* **2015**, *647*, 201–211. [CrossRef]
19. Liu, C.; Zheng, H.; Gu, X.; Jiang, B.; Liang, J. Effect of severe shot peening on corrosion behavior of AZ31 and AZ91 magnesium alloys. *J. Alloys Compd.* **2019**, *770*, 500–506. [CrossRef]
20. Ortiz, A.; Tian, J.; Shaw, L.; Liaw, P. Experimental study of the microstructure and stress state of shot peened and surface mechanical attrition treated nickel alloys. *Scripta Mater.* **2010**, *62*, 129–132. [CrossRef]
21. Benedetti, M.; Fontanari, V.; Bandini, M.; Savio, E. High- and very high-cycle plain fatigue resistance of shot peened high-strength aluminum alloys: The role of surface morphology. *Int. J. Fatigue* **2015**, *70*, 451–462. [CrossRef]
22. Xiang, Y.; Liu, Y. Mechanism modelling of shot peening effect on fatigue life prediction. *Fatigue Fract. Eng. Mater. Struct.* **2009**, *33*, 116–125. [CrossRef]
23. Wagner, L. Mechanical surface treatments on titanium, aluminum and magnesium alloy. *Mater. Sci. Eng. A* **1999**, *263*, 210–216. [CrossRef]
24. Takahashi, K.; Osedo, H.; Suzuki, T.; Fukuda, S. Fatigue strength improvement of an aluminum alloy with a crack-like surface defect using shot peening and cavitation peening. *Eng. Fract. Mech.* **2018**, *193*, 151–161. [CrossRef]
25. Cho, K.T.; Song, K.; Oh, S.H.; Lee, Y.K.; Lim, K.M.; Lee, W.B. Surface hardening of aluminum alloy by shot peening treatment with Zn based ball. *Mater. Sci. Eng. A* **2012**, *543*, 44–49. [CrossRef]
26. Moshtaghi, M.; Sato, S. Characterization of dislocation evolution in cyclically loaded austenitic and ferritic stainless steels via XRD line-profile analysis. *ISIJ Int.* **2019**, *59*, 1591–1598. [CrossRef]
27. Tanaka, K. The cosα method for X-ray residual stress measurement using two-dimensional detector. *Mech. Eng. Rev.* **2019**, *6*, 18–378. [CrossRef]
28. Klug, H.P.; Alexander, L.E. *X-Ray Diffraction Procedures for Polycrystalline and Amorphous Materials*, 2nd ed.; Wiley: New York, NY, USA, 1974; p. 661.
29. Liu, G.; Lu, J.; Lu, K. Surface nanocrystallization of 316L stainless steel induced by ultrasonic shot peening. *Mater. Sci. Eng. A* **2000**, *286*, 91–95. [CrossRef]
30. Moshtaghi, M.; Safyari, M. Effect of work hardening mechanisms in asymmetrically cyclic loaded austenitic stainless steels on low-cycle and high-cycle fatigue behavior. *Steel Res. Int.* **2020**, *92*, 202000242. [CrossRef]
31. Kim, S.J.; Kim, S.K.; Park, J.C. The corrosion and mechanical properties of Al alloy 5083-H116 in metal inert gas welding based on slow strain rate test. *Surf. Coat. Technol.* **2010**, *205*, 73–78. [CrossRef]
32. Moshtaghi, M.; Safyari, M. Effect of dwelling time in VIM furnace on chemical composition and mechanical properties of a Ni–Fe–Cr alloy. *Vacuum* **2019**, *169*, 108890. [CrossRef]
33. Graf, M.; Hornbogen, E. Observation of ductile intercrystalline fracture of an Al-Zn-Mg alloy. *Acta Metall.* **1977**, *25*, 883–889. [CrossRef]

34. Moshtaghi, M.; Abbasi, S.M. Effect of vacuum degree in VIM furnace on mechanical properties of Ni−Fe−Cr based alloy. *Trans. Nonferr. Metals Soc. China* **2012**, *22*, 2124–2130. [CrossRef]
35. Han, Y.; Xue, S.; Fu, R.; Zhang, P. Effect of hydrogen content in ER5183 welding wire on the tensile strength and fracture morphology of Al–Mg MIG weld. *Vacuum* **2019**, *166*, 218–225. [CrossRef]
36. Safyari, M.; Moshtaghi, M.; Kuramoto, S. Effect of strain rate on environmental hydrogen embrittlement susceptibility of a severely cold-rolled Al–Cu alloy. *Vacuum* **2020**, *172*, 109057. [CrossRef]
37. Tadenuma, H.; Kuramoto, S.; Kobayashi, J.; Itoh, G.; Aoi, I.; Shimizu, Y. Influence of cold rolling on strength and resistance to hydrogen embrittlement in Al–8%Zn–2%Mg–2%Cu–0.15%Zr alloy. *J. Alloys Comp.* **2019**, *69*, 69–312. [CrossRef]
38. Safyari, M.; Hojo, T.; Moshtaghi, M. Effect of environmental relative humidity on hydrogen-induced mechanical degradation in an Al–Zn–Mg–Cu alloy. *Vacuum* **2021**, *184*, 109937. [CrossRef]
39. John, M.; Kalvala, P.R.; Misra, M.; Menezes, P.L. Peening techniques for surface modification: Processes, properties, and applications. *Materials* **2021**, *14*, 3841. [CrossRef]
40. Dai, S.; Zhu, Y.; Huang, Z. Microstructure and tensile behavior of pure titanium produced after high-energy shot peening. *Mater. Sci. Technol.* **2016**, *32*, 1323–1329. [CrossRef]
41. Moshtaghi, M.; Safyari, M.; Kuramoto, S.; Hojo, T. Unraveling the effect of dislocations and deformation-induced boundaries on environmental hydrogen embrittlement behavior of a cold-rolled Al–Zn–Mg–Cu alloy. *Int. J. Hydorg. Energy* **2021**, *46*, 8285–8299. [CrossRef]
42. Pressouyre, G.M. A classification of hydrogen traps in steel. *Metall. Mater. Trans. A* **1979**, *10*, 1571–1573. [CrossRef]
43. Robertson, I.M.; Sofronis, P.; Nagao, A.; Martin, M.L.; Wang, S.; Gross, D.W. Hydrogen embrittlement understood. *Metall. Mater. Trans. A* **2015**, *46*, 2323–2341. [CrossRef]
44. Ma, C.L.; Takasugi, T.; Hanada, S. Suppression of environmental embrittlement of Ni3(Si,Ti) alloys by shot peening. *Scripta Mater.* **1996**, *34*, 1131–1138. [CrossRef]
45. Danielson, M.J. Use of the Devanathan-Stachurski cell to measure hydrogen permeation in aluminum alloys. *Corrosion Sci.* **2002**, *44*, 829–840. [CrossRef]
46. Tao, N.; Sui, M.L.; Lu, J.; Lua, K. Surface nanocrystallization of iron induced by ultrasonic shot peening. *Nanostruct. Mater.* **1999**, *11*, 433–440. [CrossRef]